MAL33 drives natural variation in maltose metabolism in Saccharomyces eubayanus

Pablo Quintrel[1,2*], Felipe Muñoz-Guzmán[1,2,3*], Pablo Villarreal[2,4], Tomas A. Peña[1,2], Natalia I. Garate[1], Catalina Muñoz-Tapia[2,5,6], Christian I. Oporto[1,5], Johnathan G. Crandall[7], Luis F. Larrondo[6], Chris Todd Hittinger[7], Gilles Fischer[8] and Francisco A. Cubillos[1,2,3,5#].

[1]*Facultad de Química y Biología, Departamento de Biología, Universidad de Santiago de Chile, Santiago, 9170022, Chile.*

[2]*Millennium Institute for Integrative Biology (iBio), Santiago, 7500574, Chile.*

[3]*Centro Científico y Tecnológico de Excelencia Ciencia & Vida, Fundación Ciencia & Vida, Huechuraba, 8580702, Santiago, Chile*

[4]*Centro de Genómica y Bioinformática, Facultad de Ciencias, Ingeniería y Tecnología, Universidad Mayor, 8580745, Santiago, Chile.*

[5]*Millenium Nucleus of Patagonian Limit of Life (LiLi), Santiago, 7500574, Chile.*

[6]*Departamento Genética Molecular y Microbiología, Facultad de Ciencias Biológicas, Pontificia Universidad Católica de Chile, 8320165, Santiago, Chile.*

[7]*Laboratory of Genetics, J. F. Crow Institute for the Study of Evolution, Center for Genomic Science Innovation, Department of Energy (DOE) Great Lakes Bioenergy Research Center, Wisconsin Energy Institute, University of Wisconsin-Madison, Madison, WI 53726, USA.*

[8]*Laboratory of Computational and Quantitative Biology, CNRS, Institut de Biologie Paris-Seine, Sorbonne Université, F-75005, Paris, France.*

(*) These authors equally contributed to this work.

#Address correspondence to Francisco A. Cubillos, francisco.cubillos.r@usach.cl

Running title: Natural variation in maltose consumption across *S. eubayanus* strains

Abstract

Maltose is one of the most abundant sugars in brewer's wort, and its efficient utilization is critical for successful fermentation. However, maltose consumption varies naturally among *Saccharomyces eubayanus* strains isolated from different host trees, such as *Quercus* and *Nothofagus*. To identify the genetic determinants underlying these phenotypic differences, we performed bulk segregant analysis (BSA) and quantitative trait loci (QTL) mapping using an F_2 offspring derived from QC18 (*Quercus*-associated) and CL467.1 (Nothofagus-associated) strains. QTL mapping identified two significant genomic regions on subtelomeric loci of chromosomes V-R and XVI-L, each containing complete *MAL* loci composed of *MAL32* (encoding maltase), *MAL31* (transporter), and *MAL33* (transcriptional activator) genes. Comparative polymorphism analyses identified mutations in *MAL32* and *MAL33* of QC18, including frameshift mutations resulting in premature stop codons. Functional validation demonstrated that the heterologous expression of $MAL33_{ChrV}$ from CL467.1 fully restored maltose utilization in QC18, indicating the functional presence of *MAL33* cis-regulatory sequences and *MAL32* and *MAL31* genes in QC18. While structural protein predictions identified truncation and impaired functionality in the maltose-responsive activation domain of Mal33p from QC18, overexpression of QC18's own $MAL33_{ChrV}$ allele also improved maltose metabolism, suggesting dosage-dependent transcriptional limitations rather than complete functional loss. These results indicate that allelic variations in the maltose-responsive activation domain of Mal33p result in differences in maltose consumption between strains. We hypothesized that reduced maltose metabolism in QC18 is an adaptive response to the distinct sugar composition in *Quercus robur* bark, contrasting with the starch-rich environment of *Nothofagus pumilio*. These findings highlight subtelomeric *MAL* gene diversity as a reservoir of genetic variation, representing a key evolutionary mechanism that influences maltose adaptation among natural *Saccharomyces* isolates.

Keywords: yeast, maltose, natural variation, protein, host, evolutionary plasticity

Introduction

In *Saccharomyces* yeasts, maltose utilization is tightly controlled by the presence of the *MAL* locus (Goldenthal et al. 1987; Ohdate et al. 2018), which contains the essential genetic information for maltose metabolism (Needleman and Michels 1983; Brickwedde et al. 2018). It consists of a transcriptional activator that controls the expression of a maltose permease and an alpha-glucosidase (maltase) encoded by *MALx3*, *MALx1*, *and MALx2 genes,* respectively (Charron et al. 1989; Chow et al. 1989; Naumov et al. 1994; Brown et al. 2010). Although the *MAL* locus is typically organized in a functionally conserved locus across the *Saccharomyces* genus (Brouwers et al. 2019), its subtelomeric location makes it a hotspot for structural and regulatory variation (Brown et al. 2010; Gallone et al. 2016; Gonçalves et al. 2016). These variations can markedly influence the efficiency and regulation of maltose utilization among strains (Brown et al. 2010; Duval et al. 2010; Peter et al. 2018). While domesticated strains often carry multiple *MAL* copies for rapid maltose uptake, wild isolates typically exhibit greater diversity in their utilization of maltose, reflecting possible ecological adaptations to their natural environments. (Gonçalves et al. 2016; Nikulin et al. 2020; Hutzler et al. 2021; Molinet et al. 2022).

The genes of the *MAL* locus are repressed by glucose and activated by the presence of intracellular maltose (Hatanaka et al. 2018; Perez-Samper et al. 2018; Hatanaka et al. 2022). Glucose depletion leads to a metabolic rewiring that involves the derepression and activation of the *MAL* genes, which synthesize the necessary enzymes for utilizing maltose, thereby resuming exponential growth, a process known as the diauxic shift. The efficient utilization of maltose is a key adaptive trait in yeasts (New et al. 2014; Venturelli et al. 2015). S. *cerevisiae* strains from different populations exhibit a natural variation in maltose consumption (Warringer et al. 2011; Gonçalves et al. 2016; Caudal et al. 2024; Hernández-Vásquez et al. 2024). Depending on the yeast strain, the metabolic reprogramming involved in this trait can persist for several hours (Wang et al. 2015; Nikulin et al. 2020). In this sense, natural isolates of *Saccharomyces eubayanus*, the cold-tolerant parental species of the industrial hybrid *Saccharomyces pastorianus* (Libkind et al. 2011; Brouwers et al. 2019; Nespolo et al. 2020), tend to exhibit a slow diauxic lag phase under wort conditions, likely due to strong glucose repression (Mardones et al. 2022; Molinet et al. 2022). The ability to consume maltose is present across most sub-populations of *S. eubayanus*. Wild *S. eubayanus* isolates

from Patagonia possess two complete copies of the *MAL* locus (Brickwedde et al. 2018; Brouwers et al. 2019) and exhibit wide phenotypic variation in maltose growth and consumption, resulting in differences in their fermentative capacity (Nespolo et al. 2020; Molinet et al. 2022). However, maltose consumption is relatively absent in the Holarctic strains (Bergin et al. 2022). This may be attributed to an altered maltose expression profile in the *MAL* locus (Eizaguirre et al. 2018; Baker et al. 2019; Langdon et al. 2020; Crandall et al. 2023). Most notably, Holarctic yeasts in the Northern Hemisphere have only been isolated from *Quercus robur*, including *S. eubayanus* isolates from Ireland (Bergin et al. 2022). Notably, the QC18 strain, isolated from an exotic *Q. robur* tree in Argentina and belonging to the Patagonian A lineage, also exhibited a low fermentative profile, poor maltose consumption, and a slow adaptation to maltose in mixed media containing glucose, which can last several days (Molinet et al. 2022). Although previous work identified *CIN5* allelic variants that impact the diauxic shift between *S. eubayanus* strains, these variants did not recapitulate their phenotypic differences, suggesting that additional genetic determinants underlie the phenotypic differences between strains. In this sense, the genetic determinants underlying maltose consumption and gene expression differences across *S. eubayanus* strains remain unknown.

To elucidate the genetic basis of maltose consumption variation in *S. eubayanus*, we investigated two strains exhibiting contrasting phenotypes in beer wort fermentation and maltose consumption: CL467.1 and QC18, representing a short and long lag phase during diauxic shift experiments, respectively. To uncover the genetic factors responsible for maltose consumption during fermentation, we characterized their phenotypic response under various conditions using quantitative trait locus (QTL) analysis. Finally, a complementation assay restored the QC18 maltose consumption trait, highlighting that allelic variation in the *MAL33* transcriptional activator gene is the major driver of phenotypic differences. Additionally, we characterized the phenotypic contribution of the two *MAL* locus copies in QC18 and CL467.1 strains, demonstrating a differential contribution to the maltose consumption phenotype. These results highlight the evolutionary role of gene families in subtelomeric regions and provide a plausible ecological explanation for the natural variation in maltose consumption observed among natural *S. eubayanus* strains.

MATERIALS AND METHODS

Strains and storage media

The strains used in this work are listed in Table S1 (Molinet et al., 2022). All the strains were maintained on YPD solid media (1% yeast extract, 2% peptone, 2% glucose, 2 % agar). For long-term storage, all strains were frozen in storage media (YPD, glycerol 20%) at -80°C.

Diauxic growth phenotypic characterization

Strains were phenotypically characterized in microculture conditions in 96-well plates under different diauxic media conditions. Carbon sources and conditions are listed in Table S2. Pre-cultures were grown 24 hours on YP (1% yeast extract, 2% peptone) supplemented with 5% glucose as the only carbon source for 24 hours at 25°C. Then, the pre-culture was refreshed by diluting 20 μL of the initial culture with 180 μL of YP 5% glucose for 24 hours at 25°C. On the third day, 20 μL of the pre-culture were washed in 180 μL of YP media, and then 20 μL were inoculated to the media array of different carbon sources to a final volume of 200 μL. For the main experiment, we denominated 'sudden' and 'gradual' diauxic shift experiments if cells were incubated in a single carbon source or a mixture of carbon sources, respectively. Growth was constantly monitored every 60 minutes at OD_{620} in a TECAN sunrise instrument at 20°C. For the large-scale segregant pool phenotyping, plates were incubated on a SPECTROstar Omega plate reader (BMG Labtech) equipped with a microplate stacker, and OD_{620} was measured every hour. Biomass generation was quantified using the Area Under Curve (AUC), using the GrowthCurver package built under R software version 4.1.2. All growth measurements represent the averages of at least three biological replicates.

Generation of F1 Hybrids and F_2 segregants between CL467.1 and QC18

The CL467.1 and QC18 hybrid was constructed using a wild-type version of QC18 and a stable haploid version of CL467.1 (Molinet et al. 2022). For this, the QC18 strain was sporulated on 2% potassium acetate agar plates (2% agar) for at least seven days at 12 °C. Crosses were performed between a QC18 spore and an isolated CL4671.1 cell using a SporePlay micromanipulator (Singer, UK). Crosses were checked by colony PCR using the *HO* gene as a marker as previously described (Molinet et al. 2022). All the primers are listed in Table S3.

F_2 segregants were obtained by sporulating the F_1 CL4671.1 x QC18 Hybrid, as previously mentioned. Haploid segregants were selected by colony PCR of the *MAT* and *HO* loci (**Table S3**). A total of 273 haploids segregants were obtained and stored for future experiments. An F_2 segregant is considered transgressive if its total growth value (Area Under the Curve, AUC) is either lower or higher than the phenotypic value of the parental strain QC18 or CL467.1, respectively.

DNA extraction

DNA was obtained from an overnight 100 µL saturated culture for each segregant. Cells were treated with 10uL Zymolyase 100T (50mg/mL) at 37°C for 1 hour, and DNA extraction was performed using the Quick-DNA, Miniprep Kit (ZymoResearch). DNA concentrations were measured in Qubit (Invitrogen). 100 ng of DNA from each segregant were mixed, and two top and bottom DNA pools were generated. Whole genome sequencing of parental strains and segregant pools was performed using Illumina pair-end sequencing (Illumina NextSeq500, Universidad de Santiago de Chile).

Bioinformatic and QTL mapping analyses

Initially, reads were processed using fastp 0.23.2 (-q 20 -F 15 -f 15) (Chen et al, 2018). Trimmed reads were aligned against the *S. eubayanus* CBS12357^T reference genome (Libkind et al, 2011) using BWA-mem (option: -M -R) (https://github.com/lh3/bwa). Mapping quality, summary statistics and variant calling were performed as previously described (Peña et al. 2024). Specifically, variants were called per chromosome per sample using HaplotypeCaller (default settings). We only considered SNPs without missing data using –max-missing 1 (https://github.com/broadinstitute/gatk). Allele counts from CL4671.1 and QC18 at each polymorphic site were obtained using bcftools stats command (Danecek et al. 2021). Allele count was performed using Python 3; the Allele frequency graph was plotted using ggplot2 in R.

LOD scores for allele frequency differences between the pools were calculated using MULTIPOOL in Python 2 Version 0.10.2 (https://github.com/matted-zz/multipool). Allele counts were the input to the mp_inference.pt script in python 2; with the options -m contrast -r 100 -c 2200 -n 30. Regions with LOD score greater than 10 were deemed as QTLs.

Reciprocal hemizygosity analysis.

Null mutants were constructed using CRISPR-Cas9 (DiCarlo et al. 2013) as previously described in *S. eubayanus* (Molinet et al. 2022). Briefly, each gRNA was cloned in the plasmid pAEF5 (Fleiss et al. 2019) using a standard "Golden Gate Assembly" (Horwitz et al. 2015). A KanMX cassette was inserted within the two selected QTL blocks linked to maltose utilization for the Reciprocal hemizygosity analysis. For this, we used, in each case, two gRNAs targeting the block's extremes and a donor DNA containing a KanMX cassette flanked by 30bp sequences of the target regions. Plasmids and donor DNA were co-transformed using the Lithium acetate protocol (Baker et al., 2019). Correct gene deletion was confirmed by standard colony PCR. All the primers, gRNAs and donor DNA are listed in **Table S3.** Reciprocal hemizygotes were constructed by crossbreeding one wild type strain against another containing the mutated target gene. All the strains generated are listed in Table S1.

Episomal heterologous complementation assay

The *S. cerevisiae* laboratory strain BY4741 was used to assemble the expression plasmid pRS426 (Christianson et al. 1992). A DNA fragment containing overlapping regions with the vector, the *MAL33* ORF, and the immediate 1 kb upstream region of the *MAL33* transcriptional starting site from chromosomes V and XVI from QC18 and CL467.1 strain were amplified by PCR (**Table S3**). The pRS426 plasmid was linearized using the Kpn*I* and EcoR*I* enzymes (NEB, UK) at 37°C for 3 hours, followed by inactivation at 80°C for 20 minutes. The *MAL33* gene constructs and the linearized plasmid were co-transformed into the BY4741 strain using the standard lithium acetate transformation protocol, with uracil as the transformant selection agent. Plasmids were extracted using the Zymoprep yeast miniprep kit II (Zymo Research) and transformed into *DH5-*α competent *Escherichia coli* strains using a standard transformation protocol (Kostylev et al. 2015). Purified plasmids were transformed into the corresponding *S. eubayanus* strain, using Geneticin (G418) as a selection marker.

Protein structure prediction

To predict the tertiary structure of the Mal33 regulatory protein from both QC18 and CL467.1 genomes, we utilize the ColabFold notebook, a Google Colab-based AlphaFold2 (Mirdita et al. 2022). Protein sequences translated from FASTA files of *MAL33*$_{ChrV}$ and *MAL33*$_{ChrXVI}$ from QC18 and CL467.1 strains were used as input. For each protein prediction we use the developer's best practices recommendation (Kim et al. 2025).

Multiple sequence alignments (MSA) were generated using MMseqs2 against UniRef and environmental databases, and template search was enabled to include PDB70-derived templates. The AlphaFold2 pipeline was executed using the five standard pre-trained models, with default settings including three recycling cycles and Amber-based structural relaxation. Each protein generated five models ranked by confidence score pLDDT, and the top-ranked model (rank 1) was selected and exported in PDB format. Finally, the selected rank 1 structure was visualized and rendered using PyMOL.

RESULTS

Maltose growth differences between S. eubayanus strains.

We systematically compared the growth of strains QC18 and CL467.1 at different maltose concentrations. Cells were first grown for 48 hours in YP medium with 5% glucose, then shifted to various maltose levels (ranging from 5% to 30%), and the progression of biomass was measured (Figure 1). Growth was evaluated by calculating the Area Under the Curve (AUC), ODmax, and lag-phase duration after 96 hours (Figure 1A). Neither strain showed significant differences in AUC and ODmax at low maltose concentrations (YP-5% maltose, *p*-value > 0.05). However, significant differences in the three analyzed parameters were evident between strains at concentrations above 5% (Figure 1B, *p*-value < 0.05). While 10% maltose also revealed distinct behaviors, the most pronounced differences in the three parameters measured occurred in YP-20% maltose. Here, the QC18 strain exhibited AUC and ODmax values that were 5.2x and 2.5x lower than CL467.1 (*p*-value < 0.05, ANOVA), respectively. Additionally, QC18 exhibited a lag phase that was 1.7x more pronounced than CL467.1 (p-value < 0.05, Table S4A), with a lag phase partial exit occurring only after 72 hours (Figure 1C). Moreover, when maltose concentration was increased to 30%, QC18 failed to grow, whereas CL467.1 exhibited only a slight reduction compared to its growth in 20% maltose, albeit a longer lag (Figure 1C). Sudden diauxic growth assays under galactose and sucrose showed only minor strain differences (Figure S1, Table S4), indicating that the metabolic divergence between QC18 and CL467.1 is specific to high maltose conditions rather than a general response to other sugars.

Next, we evaluated the strain's growth in gradual diauxic shift conditions, using a mixture of YP-1% glucose and different galactose, sucrose, or maltose concentrations. Significant differences were observed when

20% maltose was tested, with the QC18 strain exhibiting a 2-fold lower AUC than CL467.1 (p-value < 0.05). Importantly, these differences stem from QC18 displaying a significantly lower ODmax compared to CL467.1 (Figure S2A, p-value < 0.05), rather than from lag phase differences, as seen in the sudden shift assays (Figure S2A, p-value > 0.05). showing that the growth of strain CL467.1 is not affected under this condition. Slight differences in AUC were observed between QC18 and CL467.1 in glucose:sucrose and glucose:galactose (Figure S2B and C), at concentrations under 30%. At 30%, QC18 exhibited 1.1 times higher growth in sucrose and 1.3 times higher growth in galactose compared to CL467.1. (Fig S2B and C, *p*-value > 0.05, ANOVA). These results highlight strain-specific differences, primarily for maltose, in both sudden and gradual diauxic shift conditions.

QTL mapping reveals two loci associated with maltose utilization differences.

To determine the genetic origin of the phenotypic diversity between CL467.1 and QC18 strains, we initially characterized the phenotypic segregation across an F_2 population (Table S5). We generated an F_1 CL467.1 x QC18 hybrid, and from this, 273 F_2 haploid segregants were obtained in a single sporulation round (Figure 2A). We challenged this F_2 population to two diauxic shift conditions, sudden in 20% maltose and gradual in 1% glucose with 20% maltose, respectively (Figure 2B and C). As a control condition, we evaluated the growth of the segregants in 1% glucose, which showed a narrow distribution of the F_2 population (Figure S3; Coefficient of Variation, CV = 4%), confirming the absence of differential growth under this condition.

Maltose utilization exhibited distinct segregation patterns under different diauxic conditions (Figures 2 B and 2C). Under sudden shift conditions, the F_2 segregants displayed wide phenotypic variability characterized by a bimodal distribution (Figure 2D; D = 0.053, *p*-value< 0.001, Hartigan's dip test), whereas gradual shift conditions resulted in a narrower and normally distributed response (CV equal to 41% and 18%, respectively). These results suggest that sudden and gradual maltose utilization traits may have distinct genetic determinants, representing quantitative traits with phenotypic segregation within an F_2 population. We chose the sudden diauxic shift strategy for further analysis because of the greater phenotypic variability observed in the F_2 population. In this way, we identified 3 positive and 31 negative transgressive segregants, respectively (Figure 2D).

We employed a QTL mapping approach to identify the genetic variants underlying the differential maltose utilization between the parental strains (Figure 2D, Superior and Inferior Pools). For this, we selected 30 Superior and Inferior segregants, subjected them to whole-genome Illumina sequencing, and estimated the allele frequency differences between pools using the CL467.1 genome as a reference (Figure 3A, Table S6). QTL mapping revealed two major genomic regions located in the subtelomeric arms of chromosomes V and XVI ($QTL_{ChrmV\ and}$ $QTL_{ChrmXVI}$) (Figure 3A and S4). In both QTLs, the superior segregants were enriched for CL467.1 alleles, consistent with their enhanced maltose growth, whereas inferior segregants carried the QC18 variants (Figure 3B-C). These QTLs contained complete copies of the *S. eubayanus MAL* locus (*MAL31*, *MAL32*, and *MAL33*), along with isomaltase-encoding *IMA* genes (*IMA1*, *IMA2*, and *IMA4*) (Figure 3B-C, Table S7-S8). Because these QTLs are located in repetitive subtelomeric regions with reduced mapping quality (Figure S4), we chose both loci for independent functional validation to evaluate their role in the maltose utilization phenotype.

Allelic variation in Chromosome V underlies maltose consumption variation between strains.

To determine the phenotypic effect of each QTL in maltose utilization, we performed a reciprocal hemizygosity analysis between QC18 and CL467.1 strains. First, we generated strains lacking either *MAL* locus within each QTL region using a CRISPR-Cas9 mediated strategy (Figure 4A) and challenged these mutants in sudden diauxic shift in 20% maltose (Figure 4B). Deletion of the *MAL* locus on chromosome V completely abolished growth in 20% maltose in both strains despite the presence of an additional *MAL* copy on chromosome XVI (Figure 4B). The inability of one or more genes in chromosome XVI to confer maltose utilization is further supported by mutant analyses: strains lacking the MAL_{ChrXVI} locus retained growth capacity in diauxic-shift experiments with 20% maltose. Deletion of this region in CL467.1 resulted in a 0.9-fold reduction in growth compared to the wild type, whereas in QC18, we observed a mild growth increased by 1.2-fold (Figure 4B, p-value < 0.05; Table S9).

Once the *MAL* locus mutants were constructed in QC18 and CL467.1, crosses were performed between each mutant strain and its corresponding wild-type counterpart (Figure 4C). The RHs were analyzed upon sudden shifts in 20% maltose (Figure 4D), evaluating their total growth through AUC and compared to both

parents and the F_1 hybrid (Figure 4D, Table S10). RHs carrying the CL467.1 *MAL*$_{ChrV}$ locus exhibited an 11.6x greater AUC growth than the opposite RH carrying the QC18 allele (Figure 4D, Table S10), demonstrating that allelic variation within the *MAL*$_{ChrV}$ locus underlies the growth differences observed under maltose conditions, and that this QTL has a more substantial effect than the QTL identified on chromosome XVI. Analysis of individual growth parameters revealed that AUC differences among *MAL*$_{ChrV}$ RHs were primarily driven by changes in lag phase duration, with additional effects on ODmax at higher maltose concentrations (Figure S5; Table S10). On the other hand, a different trend was observed when the same approach was used for the *MAL* locus on chromosome XVI (Figure 4D). In this case, a significant 1.25-fold AUC difference between RHs was detected, with the QC18 *MAL*$_{ChrXVI}$ allele exhibiting a greater AUC (p-value < 0.05, Figure 4D). Although statistically significant, these RHs exhibited a more negligible effect across growth parameters than the observed of *MAL*$_{ChrV}$, indicating that allelic variants within *MAL*$_{ChrV}$ exert a more substantial influence on growth under high maltose concentrations than *MAL*$_{ChrXVI}$.

To identify candidate genes within the two QTL regions, we analyzed the nucleotide sequences of the *MAL* genes from each locus using SNPeff for polymorphism prediction and sequence alignments (Table S8). In general, *MAL32* and *MAL31* exhibited a high level of identity across different chromosomes in both strains (> 98%). However, when comparing the *MAL33* loci on different chromosomes, sequence identity dropped below 80%, demonstrating greater sequence divergence than the other two *MAL* genes (Table S11)**.** The allelic comparisons between QC18 and CL467.1 revealed high-impact polymorphisms affecting the protein products of *MAL* genes on both chromosomes. However, QC18's ability to grow on low maltose concentrations suggests that the enzyme encoded by *MAL32* retains functional activity. Interestingly, in *MAL33*, two and one high-impact nucleotide mutations were identified in QC18, leading to a premature stop codon (Figure 4C). In contrast, no high-impact mutations were detected in *MAL31*. The lower sequence identity between chromosome copies and premature stop codons in *MAL33* suggests that differences in transcriptional regulation may affect maltose utilization between strains.

Complementation of MAL33 transcription factor restores maltose utilization in QC18.

To validate the contribution of allelic variation in *MAL33*, we conducted a heterologous complementation assay using a multicopy episomal vector (pRS426), which is typically maintained at 20-40 copies per cell and promotes strong overexpression of the different alleles of the *MAL33* locus (Promoter-ORF-terminator) (Christianson et al. 1992; Chen et al. 2021). Total growth was assessed upon a sudden diauxic shift to 20% maltose. In strain CL467.1, none of the variants ectopically expressing *MAL33* outperformed the wild-type strain, thus confirming the inherently high functional performance of the wild-type alleles (Figure 5A; Table S12). However, in QC18, the heterologous expression of *the MAL33$_{ChrV}$* allele from CL467.1 resulted in a significant 2.7-fold AUC increase compared to the wild-type (Figure 5A), indicating that the expression of a functional transcriptional activator alone restores the QC18 ability to grow in high maltose concentrations. Similarly, overexpressing the native *MAL33*$_{ChrV}$ allele in QC18 significantly increases its growth by 2.2-fold (Figure 5B), indicating that the protein encoded by this allele is functional, thereby reinstating the maltose consumption phenotype in this strain ($p < 0.05$, ANOVA). These findings suggest that, despite nucleotide-level predictions of impaired functionality, the *MAL33$_{ChrV}$* allele from QC18 can activate downstream maltose-related genes. Thus, the slow growth phenotype may result from regulatory mechanisms or gene dosage effects. Interestingly, the overexpression of its own *MAL33$_{ChrXVI}$* partly restored the maltose adaptation phenotype in QC18, resulting in a 1.23-fold increase in growth, whereas overexpression of the CL467 allele failed to produce any noticeable change (Figure 5B, $p < 0.05$, ANOVA); however, these growth values remained significantly lower than those obtained with *MAL$_{ChrV}$* variants.

Based on these results, we analyzed the protein structures encoded by the different *MAL33*$_{ChrV}$ variants. This analysis revealed that QC18 encodes a truncated protein of 347 amino acids (out of a total of 471), comprising only two of the three major functional domains (Figure 5C). The first domain, encompassing a DNA-binding domain containing zinc fingers, is located near the N-terminus at residue 45. The second is a transactivation domain that spans residues 60 to 283. The QC18 *MAL33$_{ChrV}$* lacks the third domain, the maltose-responsive activation domain at the protein's C-terminus. AlphaFold modeling confirmed the truncation in the maltose-responsive domain (Figure 5C). Despite this truncation, the transactivation domain retains structural similarity to Mal33p from CL467.1, suggesting that Mal33p from QC18 remains partially functional (Figure 5D). However, we found a distinct folding pattern in the DNA-binding domain between alleles. The absence of the maltose-responsive domain and structural differences in the DNA-

binding domain likely contribute to the phenotypic differences observed between strains under maltose growth conditions. Overall, these results suggest that allelic variation in *MAL33*$_{ChrV}$, particularly in the maltose-responsive activation domain, underlies the phenotypic differences observed between CL467.1 and QC18 strains.

DISCUSSION

In this work, we identified two loci associated with differences in maltose metabolism, located in the subtelomeric regions of chromosomes V-R and XVI-L, both of which contain complete copies of the *MAL* genes (Brouwers et al., 2019). Moreover, our results indicate that natural variation in maltose consumption in *S. eubayanus* is mainly determined by hypomorphic alleles of the transcriptional activator *MAL33*, located in the subtelomeric region of chromosome V. Subtelomeric regions are known to represent hotspots for metabolic gene evolution in yeast and environmental adaptation, often exhibiting high variability and gene content variation that contributes to niche adaptation (Lambie and Roeder 1986; Linardopoulou et al. 2005; Cohn et al. 2006; Rudd et al. 2007; Barton et al. 2008; Keeney 2008; Brown et al. 2010; Teste et al. 2010; Snoek et al. 2014; Walther et al. 2014; Yue et al. 2017). Although our QTL mapping approach identified two major loci associated with maltose utilization, the widespread differences in allele frequencies across the genome suggest that this trait is not strictly monogenic. Maltose metabolism is a complex phenotype influenced by glucose repression, carbon sensing, and transcriptional regulation, and is therefore likely affected by multiple genetic modifiers with smaller individual effects (Molinet et al., 2022). In this sense, natural variation in maltose metabolism among natural strains may not be mainly driven by genes previously linked to respiration and glucose repression, such as *HAP5*, *HAP4*, *CIN5*, *PUT3*, *MIG1*, and *SNF1*, since these were not found in our analysis (Perez-Samper et al. 2018; Molinet et al. 2022).

The transition between carbon sources slows down cellular growth for the duration required to activate the expression of genes involved in utilizing alternative sugars (New et al. 2014; Pontes et al. 2024). The phenotypic differences in maltose utilization between QC18 and CL467.1 under sudden shift conditions indicate a specific defect in the maltose regulatory pathway, rather than general differences in glucose repression. This conclusion is supported by the minimal growth differences observed between strains in the

gradual shift experiments, as well as on sucrose and galactose. Since these sugars are also transported by maltose permeases (Botman et al. 2024), differences in maltose transport should be reflected in differences in sucrose transport and consumption, which was not the case, suggesting that differences in *MAL32* or *MAL33* could underlie the differences in maltose metabolism. Our results indicate that hypomorphic alleles of the *MAL33* gene are responsible for these differences, as the Mal33p protein from chromosome V would be unable to respond rapidly to maltose and efficiently activate the *MAL* genes, explaining QC18 long lag phase and poor growth when maltose concentration is above 20% compared to CL467.1. Because *MAL* loci are highly similar in sequence and located in subtelomeric regions, short-read mapping can be affected by cross-mapping. To address this limitation, we complemented the QTL mapping strategy with reciprocal hemizygosity analysis, which directly demonstrated a strong phenotypic contribution of $MAL33_{ChrV}$ and a relatively minor effect of the chromosome XVI locus. Together, QTL mapping, reciprocal hemizygosity, and targeted functional assays converge to validate the presence of two genetically distinct *MAL*-associated QTLs, with the chromosome V locus representing the major and context-independent contributor to maltose utilization.

Polymorphism analysis of *MAL* genes between QC18 and CL467.1 revealed several high-impact mutations in *MAL32* and *MAL33* alleles in QC18, including frameshift mutations leading to premature stop codons. These mutations likely result in truncated maltase and transcriptional activator proteins, consistent with previous studies showing that loss-of-function mutations in *MAL* genes from Holarctic *S. eubayanus* strains severely impair maltose metabolism (Peris et al. 2016; Brouwers et al. 2019; Bergin et al. 2022). Fermentative environments have exerted selective pressure on the *MAL* genes of yeasts such as *S. cerevisiae* and *S. pastorianus*, driving changes in their ability to sense, transport, and metabolize maltose (Gonçalves et al. 2016; Peris et al. 2023; Hernández-Vásquez et al. 2024). This supports that the increase in the copy number of these subtelomeric genes is a feature of domestication and evolution (Brown et al. 2010; Gallone et al. 2016; Ohdate et al. 2018). However, our study provides evidence of how this trait varies across natural isolates unrelated to anthropogenic environments. In this sense, in *Saccharomyces cerevisiae*, each *MAL* locus, despite having the same structure, is genetically unlinked (Needleman and Michels 1983; Ohdate et al. 2018) and has a different impact on maltose consumption (Day et al. 2002; Nijkamp et al. 2012; Gonçalves et al. 2016; Meurer et al. 2017; Weller et al. 2023). Similarly, in *S.*

eubayanus, we found that the *MAL* locus on chromosome V makes a greater contribution to the maltose adaptation phenotype than the copy on chromosome XVI. Our findings suggest that the *MAL* locus on Chromosome XVI is not sufficient to confer maltose consumption or adaptation.

Differences in regulation are a known source of phenotypic variation among strains of the same species (Hernández-Vásquez et al. 2024). An example of this is observed in the laboratory strains W303 and S288C of *S. cerevisiae*, as well as in sake strains, which are unable to consume maltose due to defects in the Mal33 regulatory protein (Nijkamp et al. 2012; Ohdate et al. 2018). This phenotype is restored through overexpression of the *MAL33* gene from maltose-consuming strains (Brown et al. 2010; Weller et al. 2023). Heterologous expression of the *MAL33*$_{ChrV}$ gene from CL467.1 in the QC18 strain restores the maltose adaptation phenotype, confirming that the *MAL31* and *MAL32* genes in QC18, along with their *cis*-regulatory sequences, are transcriptionally functional. Interestingly, QC18 also restores maltose growth when heterologously expressing its allele of *MAL33*$_{ChrV}$, indicating that the slow maltose consumption would be due to the *MAL33*$_{ChrV}$ allele encoding a hypomorphic version of this protein, with a decreased capacity to sense maltose but still able to activate the *MAL* locus. In contrast, overexpressing either *MAL33*$_{ChrXVI}$ allele failed to restore the maltose growth phenotype in QC18 fully. While the QC18 allele increased growth, it did not reach CL467.1 levels, suggesting its truncated protein may act as a hypomorph that interferes with transcription, as it lacks its maltose-response and transactivation domains (Figure S6). Furthermore, the CL467.1 *MAL33*$_{ChrXVI}$ allele also did not rescue the phenotype, with 3D structure predictions indicating an altered DNA-binding domain configuration that likely impairs *MAL* gene promoter activation. Thus, functional deficiencies in both *MAL33*$_{ChrXVI}$ activators could explain the minimal contribution of the maltose utilization trait. Protein structure prediction supports an impairment in the maltose-responsive domain at the protein's C-terminal in Mal33p in QC18 (Wang and Needleman 1996; Hu et al. 1999; Ohdate et al. 2018). In this regard, the inability of certain *S. cerevisiae* strains to consume and ferment maltose is the result of missense mutations or deletions that affect the maltose-responsive domain located at the C-terminal end (Gibson et al. 1997; Danzi et al. 2000; Danzi et al. 2003; Brown et al. 2010; Ohdate et al. 2018; Weller et al. 2023). Similarly, Holarctic *S. eubayanus* strains are unable to consume maltose due to multiple variants in the *MAL* locus, including *MAL33* (Bergin et al. 2022). Consequently, the QC18 *MAL33*$_{ChrV}$ gene would be unable to activate the maltose utilization pathway due to a dosage-dependent effect, which is alleviated

only by the heterologous expression of these genes. Together with the sequence analysis of the *MAL33*$_{ChrV}$ gene, It is possible to infer that this activator has partially lost its functionality and its capacity to respond to intracellular maltose (Change et al. 1988; Gibson et al. 1997), as the gene product still contains the DNA-binding domain and the transactivation domain (Wang and Needleman 1996; Hu et al. 1999). Considering that the maltose sensor has not yet been identified, the maltose-responsive domain of the Mal33p protein represents a candidate responsible for modulating and explaining the differences observed in maltose consumption and utilization. (Wang et al. 2002; Horák 2013).

Mutations in *MAL33*$_{ChrV}$ may have arisen recently, as *Quercus robur* is an introduced species in the Southern Hemisphere within the past 500 years and represents an exotic tree within the Patagonian forest (Haneca et al. 2009). Notably, all the known Holarctic *S. eubayanus* strains isolated in the Northern Hemisphere from *Quercus robur* trees have lost their ability to grow and consume maltose (Peris et al. 2016; Brouwers et al. 2019; Bergin et al. 2022; Crandall et al. 2023), suggesting a convergent phenotypic adaptation associated with oak trees. The low ability of QC18 to metabolize maltose might be influenced by the sugar composition of *Q. robur* bark, which primarily consists of glucose and xylose (Miranda et al. 2017). This contrasts with the higher concentrations of complex sugars, such as starch, found in the bark of native tree species like *Nothofagus pumilio* (Molinet et al. 2022). Thus, we hypothesized that *MAL* loci might be essential for survival in *Nothofagus* habitats, unlike in the *Quercus* environment, due to the differing environmental pressures. In this way, subtelomeric *MAL* gene diversity would represent a reservoir of standing genetic variation and a key evolutionary mechanism influencing maltose adaptation among natural *Saccharomyces* isolates. Future research would help characterize the metabolite composition of *Quercus* and *Nothofagus* trees, enabling a deeper understanding of how the host and environment modulate the genomic composition of natural *Saccharomyces* isolates across hemispheres.

DATA AVAILABILITY STATEMENT

All sequences have been deposited in the National Center for Biotechnology Information (NCBI) as a Sequence Read Archive under the BioProject accession number PRJNA1314239. Strains are available upon request to the corresponding author.

ACKNOWLEDGMENTS

We thank Valentina Abarca for the technical support, PQ acknowledges Hittinger Lab and Biology of Genomes Laboratory for providing infrastructure, laboratory space, and experiment equipment.

FUNDING

This research was funded by Agencia Nacional de Investigación y Desarrollo (ANID) FONDECYT program and ANID-Programa Iniciativa Científica Milenio – ICN17_022 and NCN2024_040. FC is supported by FONDECYT grant N° 1220026. PQ is supported by ANID BECAS DOCTORADO NACIONAL Folio 21201057 and Facultad de Química y Biología, Universidad de Santiago de Chile. FMG is supported by FONDECYT POSTDOCTORADO grant N°3220597 and PV by FONDECYT INICIACIÓN grant N°11240649. FC, PV and GF are funded by PROGRAMA DE COOPERACIÓN CIENTÍFICA ECOS-ANID ECOS180003 and C23B05. Research in the Hittinger Lab is funded by the National Science Foundation (DEB-2110403), USDA National Institute of Food and Agriculture (Hatch Project 7005101), and in part by the DOE Great Lakes Bioenergy Research Center (DOE BER Office of Science DE–SC0018409) The funders had no role in study design, data collection and interpretation, or the decision to submit the work for publication.

CONFLICT OF INTEREST

The other authors declare no conflicts of interest.

AUTHOR CONTRIBUTIONS

Conceptualization, P.Q, F.M.G and F.A.C; Methodology, P.Q, F.M.G, N.G, J.G.C and C.M.T; Software P.Q, T.A.P, P.V; Validation, P.Q, F.M.G; Formal analysis, P.Q; F.M.G, G.F and F.A.C; Investigation, P.Q, F.M.G, N.G and C.M.T; Resources, F.A.C, L.F.L, C.T.H and G.F; Data curation, P.Q, F.M.G and F.A.C; Visualization, P.Q and F.M.G; Supervision, F.A.C, L.F.L, C.T.H and G.F; Writing – Original Draft, P.Q, F.M.G, and F.A.C; Writing – review & editing, P.Q, F.M.G, L.F.L, C.T.H, G.F and F.A.C; Funding acquisition, F.A.C and L.F.L Project administration, F.A.C. All authors have read and agreed to the published version of the manuscript.

REFERENCES

Baker EP, Peris D, Moriarty RV, Li XC, Fay JC, Hittinger CT. 2019. Mitochondrial DNA and temperature tolerance in lager yeasts. Science Advances. 5(1):eaav1869. doi:10.1126/sciadv.aav1869.

Barton AB, Pekosz MR, Kurvathi RS, Kaback DB. 2008. Meiotic recombination at the ends of chromosomes in *Saccharomyces cerevisiae*. Genetics. 179(3):1221–1235. doi:10.1534/genetics.107.083493.

Bergin SA, Allen S, Hession C, Ó Cinnéide E, Ryan A, Byrne KP, Ó Cróinín T, Wolfe KH, Butler G. 2022. Identification of European isolates of the lager yeast parent *Saccharomyces eubayanus*. FEMS Yeast Research. 22(1):foac053. doi:10.1093/femsyr/foac053.

Botman D, Kanagasabapathi S, Rep MI, Van Rossum K, Tutucci E, Teusink B. 2024. cAMP in budding yeast: also a messenger for sucrose metabolism? Biochimica et Biophysica Acta (BBA) - Molecular Cell Research. 1871(5):119706. doi:10.1016/j.bbamcr.2024.119706.

Brickwedde A, Brouwers N, Van Den Broek M, Gallego Murillo JS, Fraiture JL, Pronk JT, Daran J-MG. 2018. Structural, physiological and regulatory analysis of maltose transporter genes in *Saccharomyces eubayanus* CBS 12357T. Frontiers in Microbiology. 9:1786. doi:10.3389/fmicb.2018.01786.

Brouwers N, Brickwedde A, Gorter de Vries AR, van den Broek M, Weening SM, van den Eijnden L, Diderich JA, Bai F-Y, Pronk JT, Daran J-MG. 2019. Himalayan *Saccharomyces eubayanus* genome sequences reveal genetic markers explaining heterotic maltotriose consumption by *Saccharomyces pastorianus* hybrids. Applied and Environmental Microbiology. 85(22):e01516-19. doi:10.1128/AEM.01516-19.

Brown CA, Murray AW, Verstrepen KJ. 2010. Rapid expansion and functional divergence of subtelomeric gene families in yeasts. Current Biology. 20(10):895–903. doi:10.1016/j.cub.2010.04.027.

Caudal É, Loegler V, Dutreux F, Vakirlis N, Teyssonnière É, Caradec C, Friedrich A, Hou J, Schacherer J. 2024. Pan-transcriptome reveals a large accessory genome contribution to gene expression variation in yeast. Nature Genetics. 56(6):1278–1287. doi:10.1038/s41588-024-01769-9.

Change YS, Dubin RA, Perkins E, Forrest D, Michels CA, Needleman RB. 1988. *MAL63* codes for a positive regulator of maltose fermentation in *Saccharomyces cerevisiae*. Current Genetics. 14(3):201–209. doi:10.1007/BF00376740.

Charron MJ, Read E, Haut SR, Michels CA. 1989. Molecular evolution of the telomere-associated *MAL* loci of *Saccharomyces*. Genetics. 122(2):307–316. doi:10.1093/genetics/122.2.307.

Chen Y, Liang J, Chen Z, Wang B, Si T. 2021. Genome-scale screening and combinatorial optimization of gene overexpression targets to improve cadmium tolerance in *Saccharomyces cerevisiae*. Frontiers in Microbiology. 12:662512. doi:10.3389/fmicb.2021.662512.

Chow THC, Sollitti P, Marmur J. 1989. Structure of the multigene family of *MAL* loci in *Saccharomyces*. Molecular and General Genetics MGG. 217(1):60–69. doi:10.1007/BF00330943

Christianson TW, Sikorski RS, Dante M, Shero JH, Hieter P. 1992. Multifunctional yeast high-copy-number shuttle vectors. Gene. 110(1):119–122. doi:10.1016/0378-1119(92)90454-W.

Cohn M, Liti G, Barton DB. 2006. Telomeres in fungi. In: Sunnerhagen P, Piskur J, editors. Comparative Genomics. p. 101–130. doi:10.1007/4735_108.

Crandall JG, Fisher KJ, Sato TK, Hittinger CT. 2023. Ploidy evolution in a wild yeast is linked to an interaction between cell type and metabolism. PLOS Biology. 21(11):e3001909. doi:10.1371/journal.pbio.3001909.

Danecek P, Bonfield JK, Liddle J, Marshall J, Ohan V, Pollard MO, Whitwham A, Keane T, McCarthy SA, Davies RM, Li H. 2021. Twelve years of SAMtools and BCFtools. GigaScience. 10(2):giab008. doi:10.1093/gigascience/giab008.

Danzi SE, Bali M, Michels CA. 2003. Clustered-charge to alanine scanning mutagenesis of the Mal63 *MAL*-activator C-terminal regulatory domain. Current Genetics. 44(4):173–183. doi:10.1007/s00294-003-0429-9.

Danzi SE, Zhang B, Michels CA. 2000. Alterations in the *Saccharomyces MAL*-activator cause constitutivity but can be suppressed by intragenic mutations. Current Genetics. 38(5):233–240. doi:10.1007/s002940000161.

Day RE, Rogers PJ, Dawes IW, Higgins VJ. 2002. Molecular analysis of maltotriose transport and utilization by *Saccharomyces cerevisiae*. Applied and Environmental Microbiology. 68(11):5326–5335. doi:10.1128/AEM.68.11.5326-5335.2002.

DiCarlo JE, Norville JE, Mali P, Rios X, Aach J, Church GM. 2013. Genome engineering in *Saccharomyces cerevisiae* using CRISPR-Cas systems. Nucleic Acids Research. 41(7):4336–4343. doi:10.1093/nar/gkt135.

Duval EH, Alves Jr SL, Dunn B, Sherlock G, Stambuk BU. 2010. Microarray karyotyping of maltose-fermenting *Saccharomyces* yeasts with differing maltotriose utilization profiles reveals copy number variation in genes involved in maltose and maltotriose utilization. Journal of Applied Microbiology. 109(1):248–259. doi:10.1111/j.1365-2672.2009.04656.x.

Eizaguirre JI, Peris D, Rodríguez ME, Lopes CA, De Los Ríos P, Hittinger CT, Libkind D. 2018. Phylogeography of the wild Lager-brewing ancestor (*Saccharomyces eubayanus*) in Patagonia. Environmental Microbiology. 20(10):3732–3743. doi:10.1111/1462-2920.14375

Fleiss A, O'Donnell S, Fournier T, Lu W, Agier N, Delmas S, Schacherer J, Fischer G. 2019. Reshuffling yeast chromosomes with CRISPR/Cas9. PLOS Genetics. 15(8):e1008332. doi:10.1371/journal.pgen.1008332.

Gallone B, Steensels J, Prahl T, Soriaga L, Saels V, Herrera-Malaver B, Merlevede A, Roncoroni M, Voordeckers K, Miraglia L, Teiling C, Steffy B, Taylor M, Schwartz A, Richardson T, White C, Baele G, Maere S, Verstrepen KJ. 2016. Domestication and Divergence of *Saccharomyces cerevisiae* Beer Yeasts. Cell. 166(6):1397-1410.e16. doi:10.1016/j.cell.2016.08.020.

Gibson AW, Wojciechowicz LA, Danzi SE, Zhang B, Kim JH, Hu Z, Michels CA. 1997. Constitutive mutations of the *Saccharomyces cerevisiae MAL* -activator genes *MAL23, MAL43, MAL63* , and *mal64*. Genetics. 146(4):1287–1298. doi:10.1093/genetics/146.4.1287.

Goldenthal MJ, Vanoni M, Buchferer B, Marmur J. 1987. Regulation of *MAL* gene expression in yeast: Gene dosage effects. Molecular and General Genetics MGG. 209(3):508–517. doi:10.1007/BF00331157.

Gonçalves M, Pontes A, Almeida P, Barbosa R, Serra M, Libkind D, Hutzler M, Gonçalves P, Sampaio JP. 2016. Distinct Domestication Trajectories in Top-Fermenting Beer Yeasts and Wine Yeasts. Current Biology. 26(20):2750–2761. doi:10.1016/j.cub.2016.08.040.

Haneca K, Katarina Čufar, Beeckman H. 2009. Oaks, tree-rings and wooden cultural heritage: a review of the main characteristics and applications of oak dendrochronology in Europe. Journal of Archaeological Science. 36(1):1–11. doi:10.1016/j.jas.2008.07.005.

Hatanaka H, Mitsunaga H, Fukusaki E. 2018. Inhibition of *Saccharomyces cerevisiae* growth by simultaneous uptake of glucose and maltose. Journal of Bioscience and Bioengineering. 125(1):52–58. doi:10.1016/j.jbiosc.2017.07.013.

Hatanaka H, Toyonaga H, Ishida Y, Mizohata E, Ono E. 2022. Functional diversity and plasticity in the sugar preferences of *Saccharomyces MALT* transporters in domesticated yeasts. FEMS Yeast Research. 22(1):foac055. doi:10.1093/femsyr/foac055.

Hernández-Vásquez CI, García-García JH, Pérez-Ortega ER, Martínez-Segundo AG, Damas-Buenrostro LC, Pereyra-Alférez B. 2024. Expression patterns of *Mal* genes and association with differential maltose and maltotriose transport rate of two *Saccharomyces pastorianus* yeasts. Applied and Environmental Microbiology. 90(7):e00397-24. doi:10.1128/aem.00397-24.

Horák J. 2013. Regulations of sugar transporters: insights from yeast. Current Genetics. 59(1–2):1–31. doi:10.1007/s00294-013-0388-8.

Horwitz AA, Walter JM, Schubert MG, Kung SH, Hawkins K, Platt DM, Hernday AD, Mahatdejkul-Meadows T, Szeto W, Chandran SS, Newman JD. 2015. Efficient multiplexed integration of synergistic alleles and metabolic pathways in yeasts via CRISPR-CAS. Cell Systems. 1(1):88–96. doi:10.1016/j.cels.2015.02.001.

Hu Z, Gibson AW, Kim JH, Wojciechowicz LA, Zhang B, Michels CA. 1999. Functional domain analysis of the *Saccharomyces MAL*-activator. Current Genetics. 36(1–2):1–12. doi:10.1007/s002940050466.

Hutzler M, Michel M, Kunz O, Kuusisto T, Magalhães F, Krogerus K, Gibson B. 2021. Unique brewing-relevant properties of a strain of *Saccharomyces jurei* isolated from ash (fraxinus excelsior). Frontiers in Microbiology. 12:645271. doi:10.3389/fmicb.2021.645271.

Keeney S. 2008. Spo11 and the Formation of DNA Double-Strand Breaks in Meiosis. In: Egel R, Lankenau D-H, editors. Recombination and Meiosis. p. 81–123. doi:10.1007/7050_2007_026.

Kim G, Lee S, Levy Karin E, Kim H, Moriwaki Y, Ovchinnikov S, Steinegger M, Mirdita M. 2025. Easy and accurate protein structure prediction using ColabFold. Nature Protocols. 20(3):620–642. doi:10.1038/s41596-024-01060-5.

Kostylev M, Otwell AE, Richardson RE, Suzuki Y. 2015. Cloning should be simple: *Escherichia coli* DH5α-mediated assembly of multiple DNA fragments with short end homologies. PloS One. 10(9):e0137466. doi:10.1371/journal.pone.0137466.

Lambie EJ, Roeder GS. 1986. REPRESSION OF MEIOTIC CROSSING OVER BY a CENTROMERE (*CEN3*) IN *SACCHAROMYCES CEREVISIAE*. Genetics. 114(3):769–789. doi:10.1093/genetics/114.3.769.

Langdon QK, Peris D, Eizaguirre JI, Opulente DA, Buh KV, Sylvester K, Jarzyna M, Rodríguez ME, Lopes CA, Libkind D, Hittinger CT. 2020. Postglacial migration shaped the genomic diversity and global distribution of the wild ancestor of lager-brewing hybrids. PLOS Genetics. 16(4):e1008680. doi:10.1371/journal.pgen.1008680.

Libkind D, Hittinger CT, Valério E, Gonçalves C, Dover J, Johnston M, Gonçalves P, Sampaio JP. 2011. Microbe domestication and the identification of the wild genetic stock of lager-brewing yeast. Proceedings of the National Academy of Sciences. 108(35):14539–14544. doi:10.1073/pnas.1105430108.

Linardopoulou EV, Williams EM, Fan Y, Friedman C, Young JM, Trask BJ. 2005. Human subtelomeres are hot spots of interchromosomal recombination and segmental duplication. Nature. 437(7055):94–100. doi:10.1038/nature04029.

Mardones W, Villarroel CA, Abarca V, Urbina K, Peña TA, Molinet J, Nespolo RF, Cubillos FA. 2022. Rapid selection response to ethanol in *Saccharomyces eubayanus* emulates the domestication process under brewing conditions. Microbial Biotechnology. 15(3):967–984. doi:10.1111/1751-7915.13803.

Meurer M, Chevyreva V, Cerulus B, Knop M. 2017. The regulatable *MAL32* promoter in *Saccharomyces cerevisiae*: characteristics and tools to facilitate its use. Yeast. 34(1):39–49. doi:10.1002/yea.3214.

Miranda I, Sousa V, Ferreira J, Pereira H. 2017. Chemical characterization and extractives composition of heartwood and sapwood from *Quercus faginea*. PLOS ONE. 12(6):e0179268. doi:10.1371/journal.pone.0179268.

Mirdita M, Schütze K, Moriwaki Y, Heo L, Ovchinnikov S, Steinegger M. 2022. ColabFold: making protein folding accessible to all. Nature Methods. 19(6):679–682. doi:10.1038/s41592-022-01488-1.

Molinet J, Eizaguirre JI, Quintrel P, Bellora N, Villarroel CA, Villarreal P, Benavides-Parra J, Nespolo RF, Libkind D, Cubillos FA. 2022. Natural variation in diauxic shift between patagonian *Saccharomyces eubayanus* strains. mSystems. 7(6):e00640-22. doi:10.1128/msystems.00640-22.

Naumov GI, Naumova ES, Michels CA. 1994. Genetic variation of the repeated *MAL* loci in natural populations of *Saccharomyces cerevisiae* and *Saccharomyces paradoxus*. Genetics. 136(3):803–812. doi:10.1093/genetics/136.3.803.

Needleman RB, Michels C. 1983. Repeated Family of Genes Controlling Maltose Fermentation in *Saccharomyces carlsbergensis*. Molecular and Cellular Biology. 3(5):796–802. doi:10.1128/mcb.3.5.796-802.1983.

Nespolo RF, Villarroel CA, Oporto CI, Tapia SM, Vega-Macaya F, Urbina K, De Chiara M, Mozzachiodi S, Mikhalev E, Thompson D, Larrondo LF, Saenz-Agudelo P, Liti G, Cubillos FA. 2020. An Out-of-Patagonia migration explains the worldwide diversity and distribution of *Saccharomyces eubayanus* lineages. PLOS Genetics. 16(5):e1008777. doi:10.1371/journal.pgen.1008777.

New AM, Cerulus B, Govers SK, Perez-Samper G, Zhu B, Boogmans S, Xavier JB, Verstrepen KJ. 2014. Different levels of catabolite repression optimize growth in stable and variable environments. PLoS Biology. 12(1):e1001764. doi:10.1371/journal.pbio.1001764.

Nijkamp JF, Van Den Broek M, Datema E, De Kok S, Bosman L, Luttik MA, Daran-Lapujade P, Vongsangnak W, Nielsen J, Heijne WH, Klaassen P, Paddon CJ, Platt D, Kötter P, Van Ham RC, Reinders MJ, Pronk JT, De Ridder D, Daran J-M. 2012. De novo sequencing, assembly and analysis of

the genome of the laboratory strain *Saccharomyces cerevisiae* CEN.PK113-7D, a model for modern industrial biotechnology. Microbial Cell Factories. 11(1):36. doi:10.1186/1475-2859-11-36.

Nikulin J, Vidgren V, Krogerus K, Magalhães F, Valkeemäki S, Kangas-Heiska T, Gibson B. 2020. Brewing potential of the wild yeast species S*accharomyces paradoxus*. European Food Research and Technology. 246(11):2283–2297. doi:10.1007/s00217-020-03572-2

Ohdate T, Omura F, Hatanaka H, Zhou Y, Takagi M, Goshima T, Akao T, Ono E. 2018. *MAL73*, a novel regulator of maltose fermentation, is functionally impaired by single nucleotide polymorphism in sake brewing yeast. PLOS ONE. 13(6):e0198744. doi:10.1371/journal.pone.0198744.

Peña TA, Villarreal P, Agier N, De Chiara M, Barría T, Urbina K, Villarroel CA, Santos ARO, Rosa CA, Nespolo RF, Liti G, Fischer G, Cubillos FA. 2024. An integrative taxonomy approach reveals *Saccharomyces chiloensis* sp. nov. as a newly discovered species from Coastal Patagonia. PLOS Genetics. 20(9):e1011396. doi:10.1371/journal.pgen.1011396.

Perez-Samper G, Cerulus B, Jariani A, Vermeersch L, Barrajón Simancas N, Bisschops MMM, Van Den Brink J, Solis-Escalante D, Gallone B, De Maeyer D, Van Bael E, Wenseleers T, Michiels J, Marchal K, Daran-Lapujade P, Verstrepen KJ. 2018. The crabtree effect shapes the *Saccharomyces cerevisiae* lag phase during the switch between different carbon sources. mBio. 9(5):e01331-18. doi:10.1128/mBio.01331-18.

Peris D, Langdon QK, Moriarty RV, Sylvester K, Bontrager M, Charron G, Leducq J-B, Landry CR, Libkind D, Hittinger CT. 2016. Complex Ancestries of Lager-Brewing Hybrids Were Shaped by Standing Variation in the Wild Yeast *Saccharomyces eubayanus*. PLOS Genetics. 12(7):e1006155. doi:10.1371/journal.pgen.1006155.

Peris D, Ubbelohde EJ, Kuang MC, Kominek J, Langdon QK, Adams M, Koshalek JA, Hulfachor AB, Opulente DA, Hall DJ, Hyma K, Fay JC, Leducq J-B, Charron G, Landry CR, Libkind D, Gonçalves C, Gonçalves P, Sampaio JP, Wang Q-M, Bai F-Y, Wrobel RL, Hittinger CT. 2023. Macroevolutionary diversity of traits and genomes in the model yeast genus *Saccharomyces*. Nature Communications. 14(1):690. doi:10.1038/s41467-023-36139-2.

Peter J, De Chiara M, Friedrich A, Yue J-X, Pflieger D, Bergström A, Sigwalt A, Barre B, Freel K, Llored A, Cruaud C, Labadie K, Aury J-M, Istace B, Lebrigand K, Barbry P, Engelen S, Lemainque A, Wincker P, Liti G, Schacherer J. 2018. Genome evolution across 1,011 *Saccharomyces cerevisiae* isolates. Nature. 556(7701):339–344. doi:10.1038/s41586-018-0030-5.

Pontes A, Paraíso F, Liu Y-C, Limtong S, Jindamorakot S, Jespersen L, Gonçalves C, Rosa CA, Tsai IJ, Rokas A, Hittinger CT, Gonçalves P, Sampaio JP. 2024. Tracking alternative versions of the galactose gene network in the genus *Saccharomyces* and their expansion after domestication. iScience. 27(2):108987. doi:10.1016/j.isci.2024.108987.

Rudd MK, Friedman C, Parghi SS, Linardopoulou EV, Hsu L, Trask BJ. 2007. Elevated rates of sister chromatid exchange at chromosome ends. PLoS Genetics. 3(2):e32. doi:10.1371/journal.pgen.0030032.

Snoek T, Voordeckers K, Verstrepen KJ. 2014. Subtelomeric regions promote evolutionary innovation of gene families in yeast. In: Louis EJ, Becker MM, editors. Subtelomeres. p. 39–70. doi:10.1007/978-3-642-41566-1_3.

Teste M-A, François JM, Parrou J-L. 2010. Characterization of a new multigene family encoding isomaltases in the yeast *Saccharomyces cerevisiae*, the IMA family. Journal of Biological Chemistry. 285(35):26815–26824. doi:10.1074/jbc.M110.145946.

Venturelli OS, Zuleta I, Murray RM, El-Samad H. 2015. Population diversification in a yeast metabolic program promotes anticipation of environmental shifts. PLOS Biology. 13(1):e1002042. doi:10.1371/journal.pbio.1002042.

Walther A, Hesselbart A, Wendland J. 2014. Genome Sequence of *Saccharomyces carlsbergensis* , the World's First Pure Culture Lager Yeast. G3 Genes|Genomes|Genetics. 4(5):783–793. doi:10.1534/g3.113.010090.

Wang J, Atolia E, Hua B, Savir Y, Escalante-Chong R, Springer M. 2015. Natural variation in preparation for nutrient depletion reveals a cost–benefit tradeoff. PLOS Biology. 13(1):e1002041. doi:10.1371/journal.pbio.1002041.

Wang J, Needleman R. 1996. Removal of a Mig1p binding site converts a *MAL63* constitutive mutant derived by interchromosomal gene conversion to glucose insensitivity. Genetics. 142(1):51–63. doi:10.1093/genetics/142.1.51.

Wang X, Bali M, Medintz I, Michels CA. 2002. Intracellular maltose is sufficient to induce *MAL* gene expression in *Saccharomyces cerevisiae*. Eukaryotic Cell. 1(5):696–703. doi:10.1128/EC.1.5.696-703.2002.

Warringer J, Zörgö E, Cubillos FA, Zia A, Gjuvsland A, Simpson JT, Forsmark A, Durbin R, Omholt SW, Louis EJ, Liti G, Moses A, Blomberg A. 2011. Trait variation in yeast is defined by population history. PLoS Genetics. 7(6):e1002111. doi:10.1371/journal.pgen.1002111.

Weller CA, Andreev I, Chambers MJ, Park M, NISC Comparative Sequencing Program, Bloom JS, Sadhu MJ. 2023. Highly complete long-read genomes reveal pangenomic variation underlying yeast phenotypic diversity. Genome Research. 33(5):729–740. doi:10.1101/gr.277515.122.

Yue J-X, Li J, Aigrain L, Hallin J, Persson K, Oliver K, Bergström A, Coupland P, Warringer J, Lagomarsino MC, Fischer G, Durbin R, Liti G. 2017. Contrasting evolutionary genome dynamics between domesticated and wild yeasts. Nature Genetics. 49(6):913–924. doi:10.1038/ng.3847.

FIGURE LEGENDS

Figure 1. Effect of Alternative Carbon Sources on Sudden Diauxic Growth. **A)** Experimental set-up for sudden diauxic shift experiments screening measuring total growth of native strains of *Saccharomyces eubayanus*. Cultures grown in YPD 5% glucose are transferred to different alternative carbon sources (maltose, galactose or sucrose) at increasing concentrations (5, 10, 20, and 30%; %w/v). **B)** Growth kinetics of QC18 (Turquoise) and CL467.1 (Orange) on YP supplemented with four different maltose concentrations. Lines depict the median OD_{620nm} of three biological replicates. **C**) Three parameters were calculated for maltose growth: total growth was determined by calculating the Area Under Curve (AUC), Lag time (h), and ODmax. QC18 and CL467.1 are shown in Turquoise and Orange, respectively. Plotted values correspond to the mean value of three independent replicates for each strain. (*) represents different levels of

significance between QC18 and CL467.1 strains in one condition (* *p*-value < 0.05; ANOVA, (**) *p*-value < 0.01 and (***) *p*-value < 0.001.

Figure 2. Bulk Segregant Analysis between QC18 and CL467.1 strains under sudden and gradual diauxic shift. A) QTL mapping strategy between QC18 and CL467.1. Growth kinetics of QC18, CL467.1, F_1 hybrid, and F_2 segregants in (**B**) sudden and (**C**) gradual diauxic shift experiments, using 20% maltose as a secondary carbon source. Parentals strains QC18 and CL467.1 are represented by turquoise and orange lines. Top and bottom 30 F_2 segregants were selected from each extreme pool, F_2 Inferior and superior segregants are represented by blue and dark orange lines, respectively. Lines show the OD_{620nm} median for three biological replicates. **D)** F_2 segregants Area Under Curve (AUC) distribution in diauxic shift experiments, using maltose, galactose or glucose as the secondary carbon source. Each dot represents an F_2 segregant, turquoise and orange dots represent QC18 and CL467.1 strains; Green represents the F_1 hybrid; blue and dark orange dots represent the F_2 Inferior and Superior pools. Dots show the median AUC of three biological replicates.

Figure 3. QTL Mapping results in a QC18 x CL467.1 recombinant population. (**A**) Allele frequency changes across the genome for the Inferior Pool and Superior Pool (Turquoise and Orange, respectively). LOD Score were plotted against the genome position (Red). Allele frequency of mapped pools against (**B**) Chromosome V-R and (**C**) XVI-L for QTL_{ChrmV} and $QTL_{ChrmXVI}$, are represented with pink and blue rectangles, respectively. Candidates' genes selected for validation within each QTL are shown in the blue and red rectangles, respectively.

Figure 4. *MAL* locus validation using reciprocal hemizygosity analysis (RHA). **A**) CRISPR-Cas9 editing strategy for candidate QTL knockout generation. Specific guide RNAs targeting each QTL. *MNT2* and *MAL32* targeted for QTL_1 (Chromosome V-R) and *MAL32* and *MAL33* targeted for QTL_2 (Chromosome XVI-L). **B**) AUC for QC18 and CL467.1 wild type and mutant strains (*malΔ* for chromosomes V and XVI, respectively), under 20% maltose sudden diauxic shift. **C**) Total growth of CL467.1/QC18 reciprocal hemizygotes under sudden diauxic shift conditions using 20% maltose as a secondary carbon source. Hemizygotes lacking MAL_{ChrV} allele are represented as red and pink dots; Hemizygotes lacking MAL_{ChrXVI} allele are represented as blue and light blue dots for CL4671.1 and QC18 respectively. Plotted values correspond to the mean value of eight independent replicates for each strain. The (*) represents different levels of significance between QC18 and CL467.1 strains in one condition (* $p < 0.05$; *** $p < 0.001$; ANOVA).

Figure 5. **Heterologous complementation assay of the *MAL33* gene**. Total growth (AUC) of (**A**) CL467.1 and (**B**) QC18 strains overexpressing $MAL33_{ChrV}$ *or* $MAL33_{ChrXVI}$ gene variants. Plotted values correspond to the mean value of three independent replicates for each strain. The (*) represents different levels of significance between QC18 and CL467.1 strains in one condition (* $p < 0.05$; ANOVA). (**C**) Genetic and functional organization of the $Mal33_{ChrV}$ activator, with a premature stop codon in the QC18 background, represented as a red asterisk. The domain architecture of the $Mal33_{ChrV}$ protein is illustrated, highlighting the DNA-binding domain (DBD), transactivation domain, and maltose response domain. (**D**) Predicted 3D structure of the $Mal33_{ChrV}$ activator protein from QC18 and CL467.1 backgrounds, different domains as the DNA-binding domain (DBD), transactivation domain, and maltose are represented by red, blue, and green.

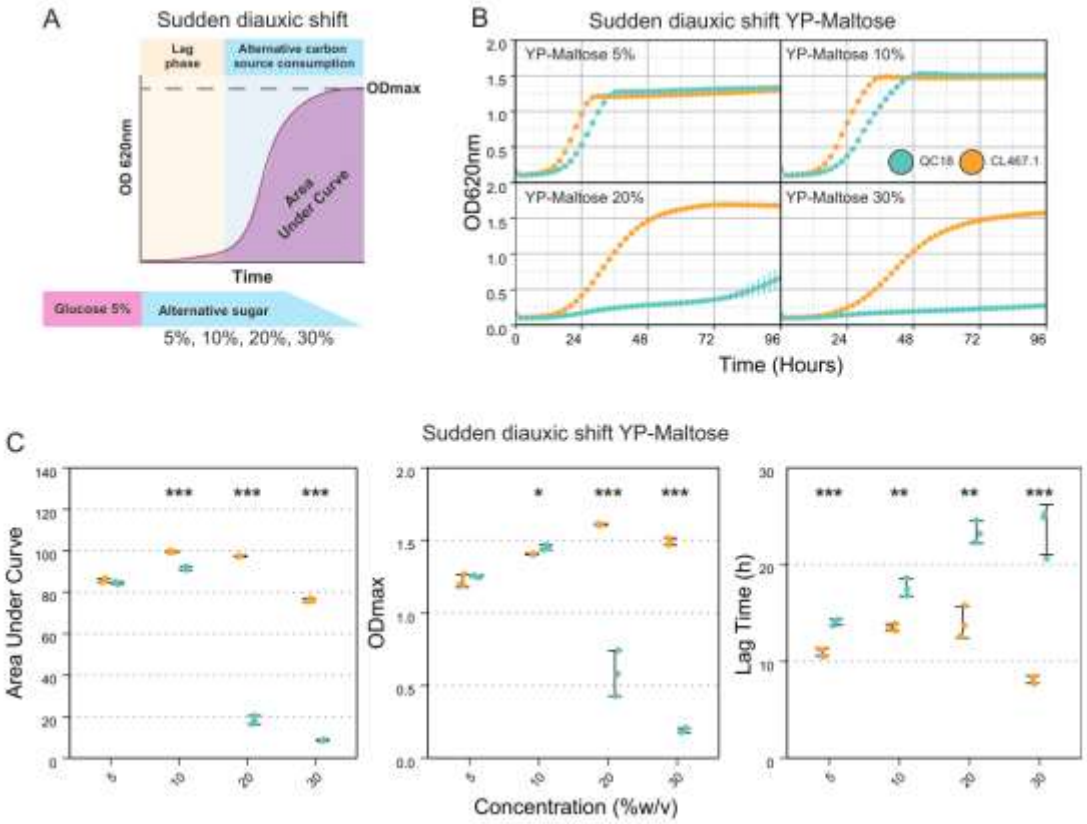

Figure 1
147x114 mm (x DPI)

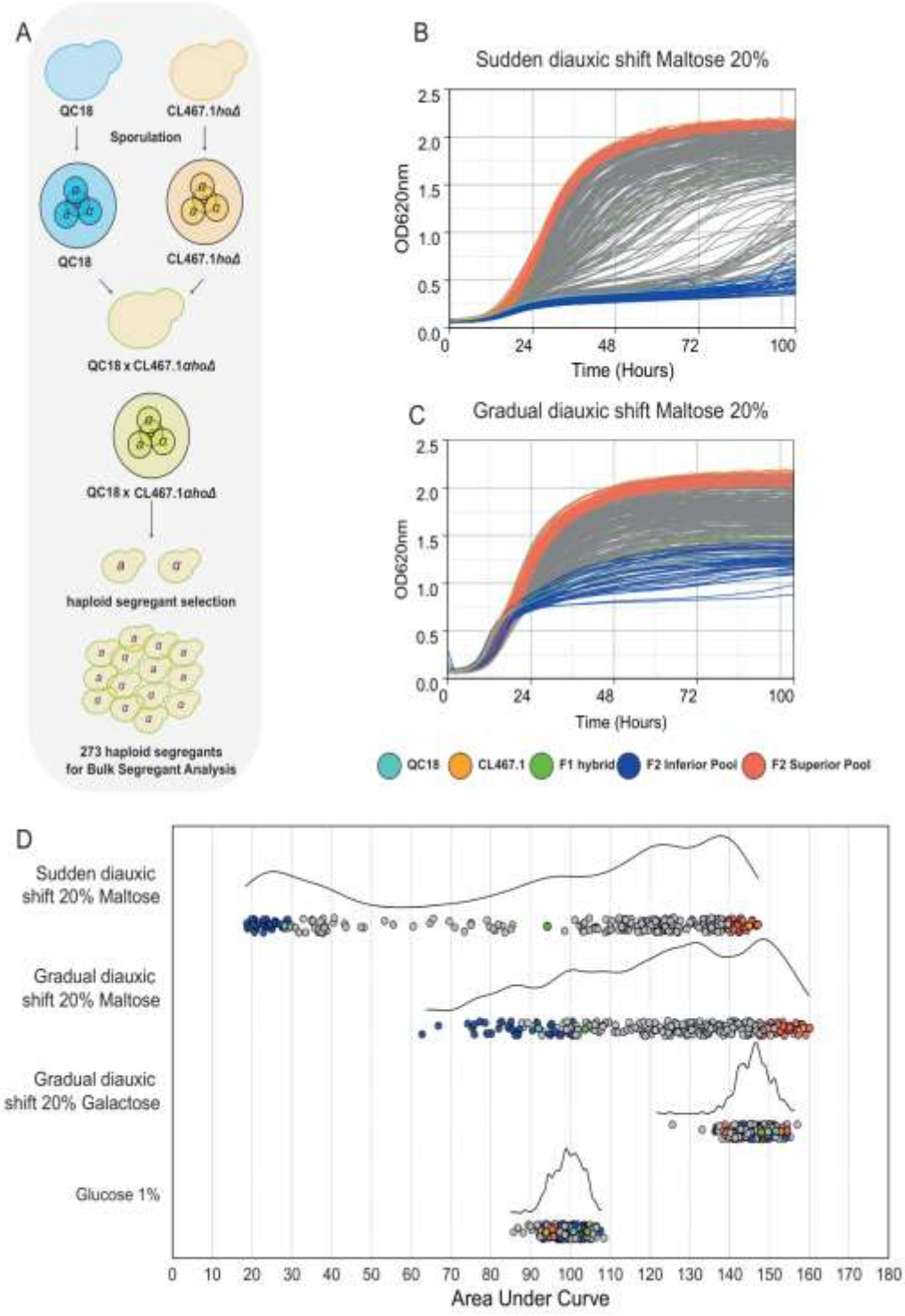

Figure 2
169x220 mm (x DPI)

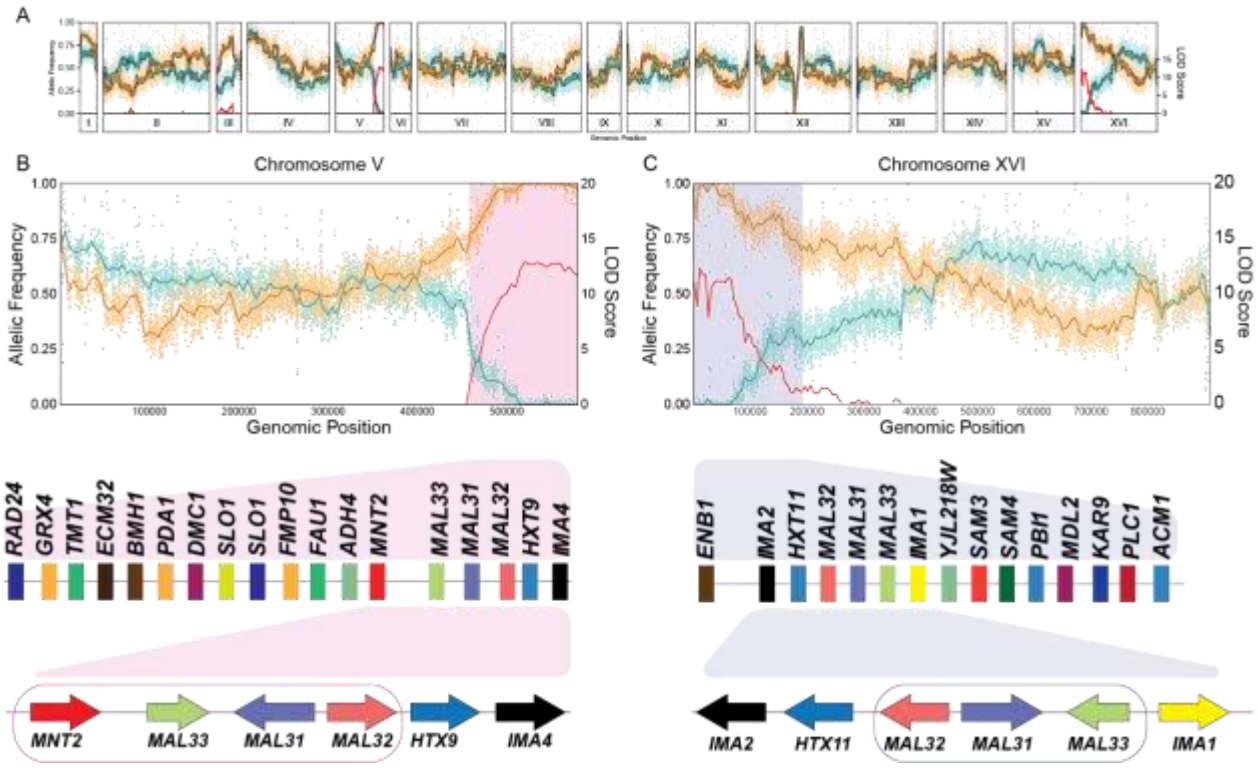

Figure 3
166x100 mm (x DPI)

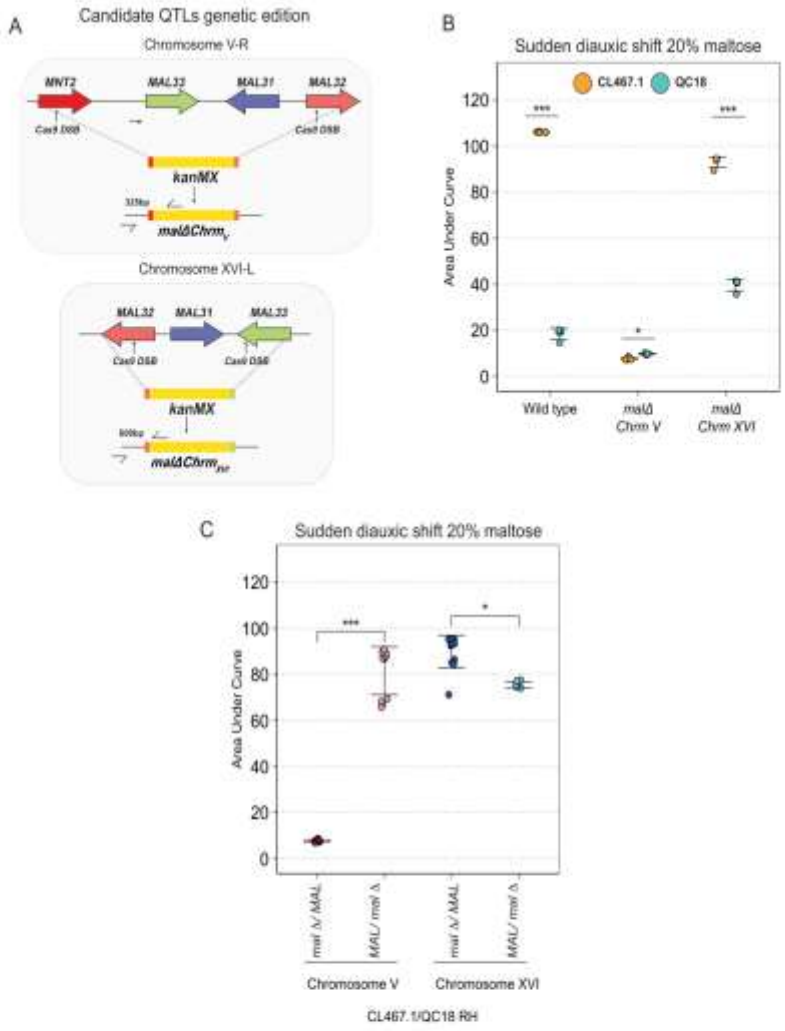

Figure 4
210x297 mm (x DPI)

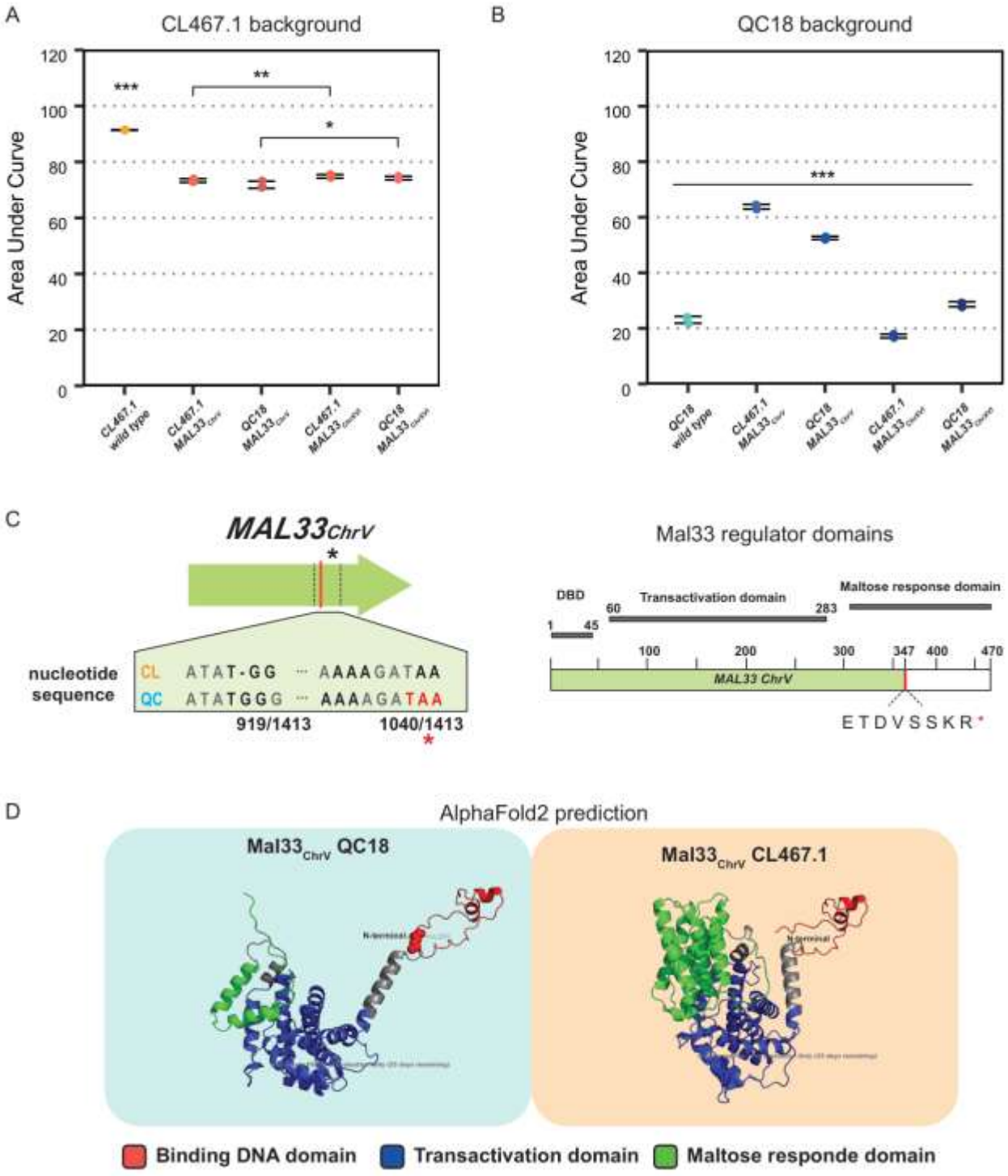

Figure 5
176x198 mm (x DPI)

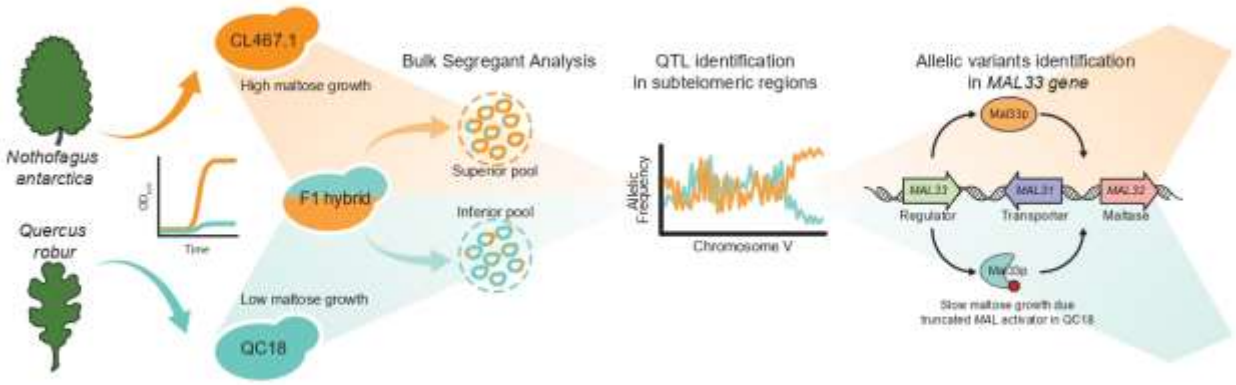

Graphical Abstract
216x279 mm (x DPI)